

## Dynamic buckling of morphoelastic filaments

Raymond E. Goldstein<sup>1,2,3,\*</sup> and Alain Goriely<sup>2,3,4</sup>

<sup>1</sup>*Department of Physics, University of Arizona, Tucson, Arizona 85721, USA*

<sup>2</sup>*BIO5 Institute, University of Arizona, Tucson, Arizona 85721, USA*

<sup>3</sup>*Program in Applied Mathematics, University of Arizona, Tucson, Arizona 85721, USA*

<sup>4</sup>*Department of Mathematics, University of Arizona, Tucson, Arizona 85721, USA*

(Received 7 February 2006; published 11 July 2006)

The equilibrium shapes of biological structures as diverse as plant tendrils and bacterial filaments can be altered by externally imposed stresses of sufficient duration. We study the simplest model for this *morphoelasticity*—a filament whose intrinsic curvatures relax to the local curvatures—and illustrate its properties in the context of dynamic Euler buckling and writhing. When a thrust or twist is ramped in time the effective elastic properties of the filament depend on the load rate. Slow ramps interrupted by removal of the external forces can leave in equilibrium any of a whole continuum of buckled shapes. Morphoelastic relaxation can also allow a filament to bypass a bifurcation.

DOI: [10.1103/PhysRevE.74.010901](https://doi.org/10.1103/PhysRevE.74.010901)

PACS number(s): 87.19.Rr, 05.45.-a, 46.35.+z, 62.40.+i

It is a familiar feature of plants that they can be trained to grow into a desired shape by external forces of sufficient duration. Viewed from the perspective of the theory of elasticity [1], this training corresponds to a change in the configuration of vanishing elastic moments. The simplest elastic energy of filaments is quadratic in the local curvatures, with a straight ground states; bent equilibria are described by introducing “intrinsic curvatures,” which feature in theories of lipid membranes [2] and bacterial flagella [3,4]. The process of training may thus be viewed as the evolution of the preferred curvatures to those encouraged by the forces. These changes arise from the addition of new material to the walls of plant cells [5] or to the peptidoglycan network of bacterial cell walls [6], or from rearrangements of interconnections within a membrane, as in the echinocytosis of erythrocytes [7]. Such structural rearrangements result in mechanical properties of these *morphoelastic* objects which depend on the dynamics of time-dependent loads, much as measurements of the strength of molecular bonds depend on the dynamics of time-dependent forces [8].

Figure 1 shows a phenomenon motivating important questions about morphoelasticity. As many climbing vines grow they produce thin, nearly straight tendrils which precess slowly around their base in a dance known as circumnutation [9,10], ready to grasp objects in their path. Within hours after its end loops around an object, a tendril develops helical regions of both hands connected by *perversions*. Existing models [11,12] view perversions as heteroclinic connections between two helical ground states in which external tension and intrinsic curvature balance. Yet, if at some intermediate time one severs the connection between the evolving filament and the plant (Fig. 1), thus removing the tension, the shape differs little from the intact one, showing that the tendril actually passes slowly through a continuum of quasi-

equilibrium states. The stability of such intermediate states without external constraints has remained unexplained. More generally, it is natural to ask: How should elasticity theory be formulated to describe morphoelasticity? How are bifurcations, such as Euler buckling and twist-induced writhing [13,14], altered by the relaxation processes? What are the effective elastic properties of such filaments under time-dependent loads? How can filament growth [15,16] be incorporated?

We study here the simplest phenomenological model of morphoelasticity, with the feature termed “viscoelasticity” [17] in the formal mechanics literature [18–23]. It has a single time scale for the relaxation of an intrinsic curvature to the actual curvature of the filament. Our focus is on shape evolution under time-dependent loads to illustrate how a filament is trained and to analyze the effective spring constant of buckled filaments as a function of load rate, a quantity amenable to direct measurement.

Consider a filament of length  $L$  and bending modulus  $A$  confined to a plane, whose shape is given by the tangent angle  $\theta(s)$  as a function of arc length  $s$ , and with clamped

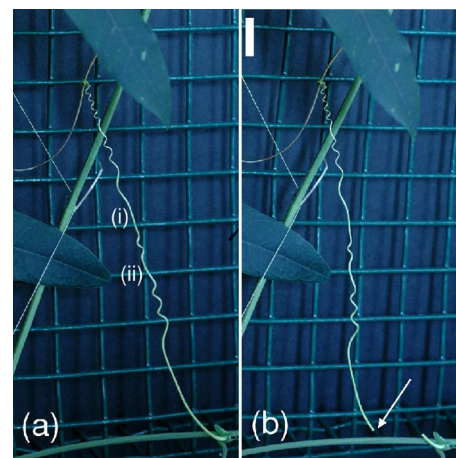


FIG. 1. (Color online) A tendril of the genus *Passiflora*. An intact tendril (a) with perversions (i), (ii) maintains its shape when its connection to the plant is cut (b, arrow). Scale bar is 1 cm.

\*Address after 1 September 2006: Department of Applied Mathematics and Theoretical Physics, Center for Mathematical Sciences, Wilberforce Road, University of Cambridge, Cambridge CB3 0WA, UK.

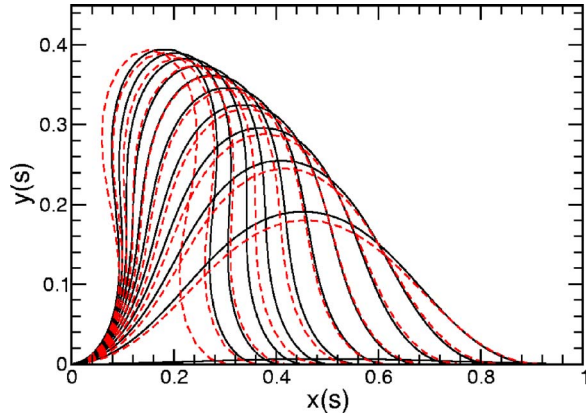


FIG. 2. (Color online) Filament shapes during a force ramp. The force  $f$  varies from 0 to 0.1, with  $r\tau=0.2$ , displayed at equal intervals. Dashed lines show analytical approximation.

boundary conditions;  $\theta(0)=\theta(L)=0$ . Let a thrusting force of magnitude  $F$  act at the two ends. With  $\kappa=\partial_s\theta$  and  $\kappa^0(s)=\partial_s\theta^0$  the signed local and intrinsic curvatures, the elastic energy is [1]

$$E[\theta]=\int_0^L ds \left( \frac{1}{2}A(\kappa-\kappa^0)^2 + F \cos(\theta) \right). \quad (1)$$

If the filament shape is  $(x(s), y(s))$ , with  $x_s=\cos(\theta)$ , the end-to-end displacement along  $x$  is  $\mathcal{L}=\int_0^L ds \cos(\theta)$ , and the second term in (1) is  $F\mathcal{L}$ , the work done by the force.

Recall the Euler buckling found when  $\theta^0=0$ . Linearization of the Euler-Lagrange equation  $A\theta_{ss}=-F\sin(\theta)$  shows that the mode  $\theta(s)=a\sin(2\pi s/L)$  sets in at a critical force  $F_c=4\pi^2A/L^2$ . Setting  $F=F_c(1+f)$ , with  $f\ll 1$ , defining the energy  $e=2(E-FL)/F_cL$ , and expanding, we obtain  $e\approx-(1/2)fa^2+(1/32)a^4+\dots$ . Minimizing  $e$  yields  $fa-(1/8)a^3=0$ , so  $a_{\pm}\approx\pm(8f)^{1/2}$ : the usual pitchfork bifurcation. Just beyond buckling the fractional compression is

$$X\equiv\frac{L-\mathcal{L}}{L}\approx\frac{a^2}{4}, \quad (2)$$

which, for this ordinary buckling problem, yields  $X\approx 2f$ . This is Hookean elasticity,  $f=kX$ , with an ideal spring constant  $k=1/2$ , or  $4\pi^2A/L^3$  in dimensionful units.

Now we generalize this problem by letting the force  $f$  be ramped in time as  $f=rt$ , and reintroduce the intrinsic curvature  $\kappa^0$  and its relaxation time  $\tau$ ,

$$\tau\frac{\partial\kappa^0}{\partial t}=\kappa-\kappa^0. \quad (3)$$

The strong separation of time scales between the relaxation of the filament geometry and the internal stresses implies that the shape can be solved in a quasistatic approximation, through the Euler-Lagrange equation

$$A(\theta_{ss}-\theta_{ss}^0)=-F\sin(\theta). \quad (4)$$

We first solve the coupled system (3) and (4) numerically, ramping from  $f=0$  to 0.1 (an upper limit within the scaling region when  $\tau\rightarrow\infty$ ), with initial amplitude  $a_0=0.01$ . A se-

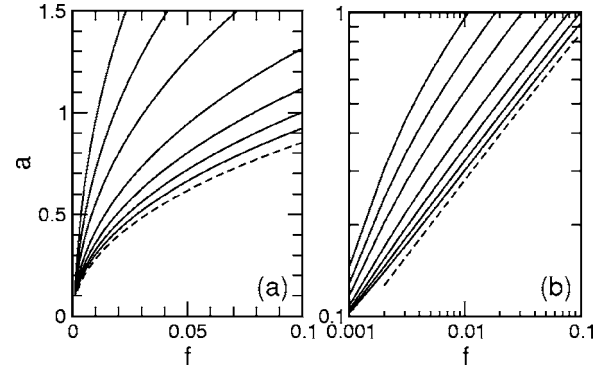


FIG. 3. Numerical results on dynamic buckling. Linear (a) and logarithmic (b) plots of mode amplitude  $a$  vs ramped force  $f$  for  $r\tau=0.05, 0.1, 0.2, 0.5, 1, 2, 5$ , and  $\infty$  (dashed).

quence of shapes is shown in Fig. 2, and a convenient order parameter, the amplitude  $a$  of the tangent angle, is shown in Fig. 3 as a function of  $f$  for various relaxation times. Figure 3(a) shows that the amplitude at a given  $f$  increases as  $\tau$  decreases, indicating “softening” of the filament. All curves [Fig. 3(b)] eventually display the  $f^{1/2}$  behavior of the pitchfork bifurcation, but with ever larger prefactors as  $\tau\rightarrow 0$ . At very small  $f$  there is a crossover associated with the finite initial value  $a_0$ .

An effective spring constant  $k_{\text{eff}}$  of the buckled filament can be estimated from the linear region of the  $f$ - $X$  curves (see Fig. 4). As  $\tau\rightarrow 0$ ,  $k_{\text{eff}}\rightarrow 0$ ; if the force ramp is infinitely slow compared to the relaxation time the intrinsic curvature relaxes to the actual curvature and there is no restoring force. To understand this, we analyze the region close to the bifurcation using  $\theta=a(t)\sin(2\pi s/L)$  and  $\theta^0=b(t)\sin(2\pi s/L)$ , leading to the system

$$rta+b-\frac{a^3}{8}=0, \quad \tau\frac{db}{dt}=a-b, \quad (5)$$

with  $a(0)=a_0$  and  $b(0)=0$ . In the fast ramp regime,  $r\tau\gg 1$ , we let  $\xi=r\tau$  and set  $\epsilon=1/r\tau$ , and (5) becomes

$$\xi a+b-\frac{a^3}{8}=0, \quad \frac{db}{d\xi}=\epsilon(a-b). \quad (6)$$

Assuming regular expansions,  $a(\xi)=a^{(0)}+\epsilon a^{(1)}+\dots$  and  $b(\xi)=b^{(0)}+\epsilon b^{(1)}+\dots$ , Eq. (6) yields  $b^{(0)}=0$  and  $a^{(0)}=(8\xi)^{1/2}$  as before, and

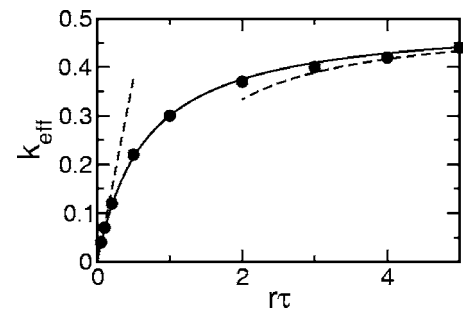


FIG. 4. Effective spring constant. Asymptotic forms (10) and (14) derived in text (dashed) compared with numerics (solid circles) and interpolating formula (solid) from Eq. (16).

$$\frac{db^{(1)}}{d\xi} = a^{(0)} - b^{(0)}, \quad \xi a^{(1)} + b^{(1)} - \frac{3a^{(0)2}a^{(1)}}{8} = 0. \quad (7)$$

Since  $b^{(0)}=0$ , we can solve immediately for  $b^{(1)}$ ,

$$b^{(1)}(\xi) = \int_0^\xi d\xi' a^{(0)}(\xi') = \frac{2\sqrt{8}}{3} \xi^{3/2}. \quad (8)$$

This yields  $a^{(1)}=b^{(1)}/2\xi=(8\xi)^{1/2}/3$ , and thus

$$a(\xi) \approx \left(1 + \frac{1}{3r\tau} + \dots\right) (8\xi)^{1/2}. \quad (9)$$

Using Eq. (2), the spring constant has the asymptotic form

$$k_{\text{eff}} = \frac{1}{2} \left(1 - \frac{2}{3r\tau} + \dots\right). \quad (10)$$

In the extreme morphoelastic limit,  $r\tau \ll 1$ , we define  $\eta = t/\tau$  with the small parameter  $\delta = r\tau$ . Then the pair (5) becomes

$$\delta\eta a + b - \frac{a^3}{8} = 0 \quad \text{and} \quad \frac{db}{d\eta} = a - b. \quad (11)$$

In the limit  $\delta \rightarrow 0$  we have  $b = a^3/8$ , hence  $(3/8)a^2 da/d\eta = a - a^3/8$ , which yields

$$a(\eta) = 8^{1/2} \left[1 - \left(1 - \frac{a_0^2}{8}\right) e^{-2\eta/3}\right]^{1/2}. \quad (12)$$

As  $\eta \rightarrow 0$ , with  $\eta \gg a_0^2/8$ , we find

$$a(\eta) \approx \frac{4}{3^{1/2}} \eta^{1/2}, \quad (13)$$

which yields the spring constant vanishing as  $\tau \rightarrow 0$ ,

$$k_{\text{eff}} \approx \frac{3}{4} r\tau + \dots. \quad (14)$$

Figure 4 shows good agreement with these two limiting cases. Inspection of these asymptotic formulas reveals that the amplitudes  $a$  and  $b$  have the same power-law time dependence in the two regimes, suggesting that an interpolating formula can be obtained through the ansatz

$$a = \alpha t^{1/2} + O(t), \quad b = \beta t^{3/2} + O(t^2). \quad (15)$$

One then deduces  $\alpha^2 = 8r + 16/3\tau$  and thus

$$k_{\text{eff}} = \frac{3r\tau}{4 + 6r\tau}, \quad (16)$$

which reproduces the limits (10) and (14) and nicely matches the numerical results over the full range of  $r\tau$ . This simple approximation to the mode dynamics also quite accurately reproduces the buckled filament shapes even far beyond the bifurcation (Fig. 2).

If the thrusting force is gradually removed at some point following a ramp, then the filament shape will soon adapt to the evolving preferred curvature and it will then be at the minimum of the elastic energy, with  $\kappa(s) = \kappa^0(s)$  everywhere. Figure 5 shows five sequences of trained shapes which result

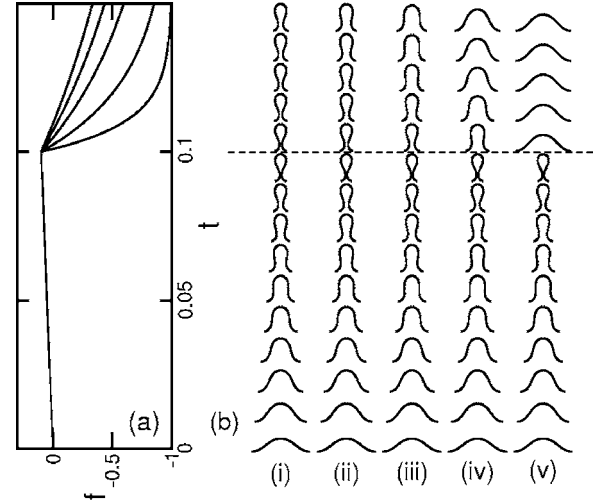


FIG. 5. Filaments trained with time-dependent forces. For each of the force-time profiles shown in (a) is the corresponding sequence of filament shapes (b) shown at intervals of  $\Delta t=0.01$ . Dashed line indicates end of linear ramp.

from a protocol of the force consisting of a ramp followed by exponential relaxation (with varying decay rates) down to  $f=-1$ , where the total thrust vanishes. As the force is removed ever more slowly, the filament remains in a more highly bent shape. Each final trained shape is typically very close to that of a nonmorphoelastic filament subjected to some particular external force, but of course the latter would not remain in place after the removal of that force. Clearly, there is no simple variational principle governing the final (history-dependent) shapes.

While the analysis above focused on properties of filaments beyond a bifurcation, morphoelasticity can also allow a system to bypass a bifurcation. A simple example is provided by the writhing instability of a twisted filament, wherein a filament of length  $L$ , bending modulus  $A$ , and twisting modulus  $C$ , clamped at both ends, is subjected to a twist  $\omega$  in the presence of a preferred twist  $\omega^0$ . If the filament is aligned along the  $z$  axis and the perpendicular displacements of the rod centerline are  $X(z)$  and  $Y(z)$ , then the equilibrium relation for the complex displacement  $\xi = X + iY$  is [1]

$$A\xi_{zzzz} - iC(\omega - \omega^0)\xi_{zzz} = 0, \quad (17)$$

with boundary conditions  $\xi(0) = \xi_z(0) = \xi(L) = \xi_z(L) = 0$ . Stability analysis shows [1] there is a critical twist  $\omega_c - \omega^0 \approx 8.98A/C$  beyond which a writhing instability will occur. Suppose now that the twist is increased gradually in time as  $\omega = \omega_c r t$ , and also that the material of the filament morphoelastically adjusts to the imposed twist by developing a preferred twist  $\omega^0$ . A simple dynamics for  $\omega^0$  is like that for the intrinsic curvature (3),

$$\tau \frac{\partial \omega^0}{\partial t} = \omega - \omega^0. \quad (18)$$

A simple calculation shows that  $\omega - \omega^0 = \omega_c r \tau (1 - e^{-t/\tau})$ ; in the long-time limit, the intrinsic twist lags behind the imposed twist by  $\omega_c r \tau$ . It follows that the writhing instability will

only occur if  $r\tau \geq 1$ , i.e., if the twist is ramped sufficiently fast or the relaxation time is sufficiently long. Otherwise, the writhing instability is completely suppressed.

The results presented here provide a basic framework for analyzing the morphoelastic properties of various biological structures. While our analysis was confined to a few particular protocols for application of time-dependent forces or torques, it is clear that a wide range of monotonic or oscillatory loading sequences, or, alternatively, specified end point positions or lateral constraints, can be explored to examine the internal relaxation rates of the intrinsic curvatures and the long-time dynamics of buckled shapes [24]. Among the most promising candidates for detailed study of this behavior are bacterial filaments [6], linear concatenations of mutant bacterial cells which fail to separate after cell division and thus remain attached end-to-end. Their relatively large lengths (exceeding hundreds of micrometers) and slow growth dynamics (hours) makes them ideally suited to study

various aspects of cell wall elasticity [25], including in particular how external forces affect the growth morphology. Such forces can be supplied by optical traps, micropipets, or confinement. Plant tendrils constitute a second important type of morphoelastic filament suited to experimental study. It is of interest to generalize the present approach to include not only uniform but also *differential* filament growth, with azimuthal variations in cell size around the filament cross section. This is suspected of playing a role in specific features of tendril perversions [26], and may manifest itself as intrinsic curvatures which grow in time.

We are grateful to Tyler McMillen, Neil Mendelson, Michael Tabor, and especially Charles Wolgemuth for important discussions, and to A. White, K. Ericsson, and R. Krug for experimental assistance. This work was supported by NSF Grants No. DMS0307427 (A.G.) and No. PHY0551742 (R.E.G.), and NIH Grant No. R01-GM72004-01 (R.E.G.).

- 
- [1] L. D. Landau and E. M. Lifshitz, *Theory of Elasticity* (Pergamon Press, Oxford, 1986).
- [2] W. Helfrich, *Z. Naturforsch. C* **28**, 693 (1973).
- [3] R. E. Goldstein, A. Goriely, G. Huber, and C. W. Wolgemuth, *Phys. Rev. Lett.* **84**, 1631 (2000).
- [4] S. V. Srigiriraju and T. R. Powers, *Phys. Rev. Lett.* **94**, 248101 (2005).
- [5] B. M. Mulder and A. M. C. Emmons, *J. Math. Biol.* **42**, 261 (2001).
- [6] N. H. Mendelson, *Microbiol. Rev.* **46**, 341 (1982).
- [7] J. K. Khodadad, R. E. Waugh, J. L. Podolski, R. Josephs, and T. L. Steck, *Biophys. J.* **70**, 1036 (1996).
- [8] E. Evans and K. Ritchie, *Biophys. J.* **72**, 1541 (1997).
- [9] C. Darwin, *The Movements and Habits of Climbing Plants* (D. Appleton, New York, 1888).
- [10] J. Sachs, *Lectures on the Physiology of Plants* (Clarendon, Oxford, 1887).
- [11] A. Goriely and M. Tabor, *Phys. Rev. Lett.* **80**, 1564 (1998).
- [12] T. McMillen and A. Goriely, *J. Nonlinear Sci.* **12**, 241 (2002).
- [13] J. H. Michell, *Messenger Math.* **11**, 181 (1889); see also A. Goriely, *J. Elast.* (to be published).
- [14] E. E. Zajac, *J. Appl. Mech.* **29**, 136 (1962).
- [15] C. W. Wolgemuth, R. E. Goldstein, and T. R. Powers, *Physica D* **190**, 266 (2004).
- [16] A. Goriely and M. Ben Amar, *Phys. Rev. Lett.* **94**, 198103 (2005).
- [17] This terminology is somewhat confusing, as the natural point of comparison for a morphoelastic material is one with ordinary elasticity, not a Newtonian fluid.
- [18] E. I. Goldengershel, *Prikl. Mat. Mekh.* **38**, 187 (1972).
- [19] E. I. Goldengershel, *Prikl. Mat. Mekh.* **40**, 766 (1975).
- [20] F. Mignot and J. P. Puel, *C. R. Seances Acad. Sci., Ser. 1* **293**, 557 (1981).
- [21] M. E. Gurtin, V. J. Nizel, and D. W. Reynolds, *J. Appl. Mech.* **49**, 245 (1982).
- [22] F. Mignot and J. P. Puel, *Arch. Ration. Mech. Anal.* **85**, 251 (1984).
- [23] D. W. Reynolds, *Proc. - R. Soc. Edinburgh, Sect. A: Math.* **99**, 371 (1985).
- [24] L. Golubovic, D. Moldovan, and A. Peredera, *Phys. Rev. E* **61**, 1703 (2000).
- [25] N. H. Mendelson, J. E. Sarlls, C. W. Wolgemuth, and R. E. Goldstein, *Phys. Rev. Lett.* **84**, 1627 (2000).
- [26] M. J. Jaffe and A. W. Galston, *Annu. Rev. Plant Physiol.* **19**, 417 (1968).